G3 Genes | Genomes | Genetics

INVESTIGATION

Ras/MAPK Modifier Loci Revealed by eQTL in *Caenorhabditis elegans*

Mark G. Sterken,* Linda van Bemmelen van der Plaat,* Joost A. G. Riksen,* Miriam Rodriguez,* Tobias Schmid,†,‡ Alex Hajnal,† Jan E. Kammenga,*,[1] and Basten L. Snoek*,[1]

*Laboratory of Nematology, Wageningen University and Research, 6708PB, The Netherlands, †Institute of Molecular Life Sciences, and ‡PhD Program in Molecular Life Sciences, University of Zurich, CH-8057, Switzerland

ORCID IDs: 0000-0001-7119-6213 (M.G.S.); 0000-0002-4098-3721 (A.H.); 0000-0003-4822-4436 (J.E.K.); 0000-0001-5321-2996 (B.L.S.)

ABSTRACT The oncogenic Ras/MAPK pathway is evolutionarily conserved across metazoans. Yet, almost all our knowledge on this pathway comes from studies using single genetic backgrounds, whereas mutational effects can be highly background dependent. Therefore, we lack insight in the interplay between genetic backgrounds and the Ras/MAPK-signaling pathway. Here, we used a *Caenorhabditis elegans* RIL population containing a gain-of-function mutation in the Ras/MAPK-pathway gene *let-60* and measured how gene expression regulation is affected by this mutation. We mapped eQTL and found that the majority (~73%) of the 1516 detected *cis*-eQTL were not specific for the *let-60* mutation, whereas most (~76%) of the 898 detected *trans*-eQTL were associated with the *let-60* mutation. We detected six eQTL *trans*-bands specific for the interaction between the genetic background and the mutation, one of which colocalized with the polymorphic Ras/MAPK modifier *amx-2*. Comparison between transgenic lines expressing allelic variants of *amx-2* showed the involvement of *amx-2* in 79% of the *trans*-eQTL for genes mapping to this *trans*-band. Together, our results have revealed hidden loci affecting Ras/MAPK signaling using sensitized backgrounds in *C. elegans*. These loci harbor putative polymorphic modifier genes that would not have been detected using mutant screens in single genetic backgrounds.

KEYWORDS
Caenorhabditis elegans
RAS/MAPK
eQTL
genetic background

The Ras/MAPK pathway is highly conserved across s metazoans and regulates a wide range of physiological responses, such as cell proliferation, apoptosis, cell differentiation, and tissue morphogenesis (Gokhale and Shingleton 2015). In humans, activating ("gain-of-function") mutations in HRas and KRas are strong tumor initiating mutations (Prior and Hancock 2012). Activation of MAP kinase components in model organisms has been shown to cause cell transformation and is implicated in tumorigenesis (Cowley *et al.* 1994; Mansour *et al.* 1994). As a key pathway in vertebrates and invertebrates, Ras/MAPK signaling has been thoroughly studied in model organisms. Genetic studies in the model nematode *Caenorhabditis elegans* have provided insight into *let-60* Ras/MAPK signaling. Activated LET-60, a member of the GTP-binding RAS family (Beitel *et al.* 1990; Han and Sternberg 1990), induces the phosphorylation of LIN-45 (a Raf ortholog), MEK-2 (a MAPK kinase), and MPK-1 (an ERK ortholog) (Wu and Han 1994). After phosphorylation, MPK-1 enters the nucleus where it regulates many genes by phosphorylation of transcription factors (Tan *et al.* 1998). Additionally, *let-60* activation underlies programmed cell death in *C. elegans* (Jiang and Wu 2014).

In *C. elegans* almost all studies on *let-60* activation have been conducted with mutant screens using single genetic backgrounds (*i.e.*, a mutation in one genotype, in this case Bristol N2). However, the phenotype of induced mutations can vary widely depending on the genetic background (Duveau and Felix 2012; Chandler *et al.* 2014; Schmid *et al.* 2015; Kammenga 2017). Induced mutations in one genetic background do not reveal the allelic effects that segregate in natural populations and contribute to phenotypic variation (Kammenga *et al.* 2008). At the moment, we lack insight into how genetic background effects modulate activated Ras/MAPK signaling and which genetic modifiers are involved in the underlying genetic architecture of gene expression.

doi: https://doi.org/10.1534/g3.117.1120
Manuscript received April 18, 2017; accepted for publication July 22, 2017; published Early Online July 27, 2017.

Supplemental material is available online at www.g3journal.org/lookup/suppl/doi:10.1534/g3.117.1120/-/DC1.
[1]Corresponding authors: Laboratory of Nematology, Wageningen University and Research, Droevendaalsesteeg 1, 6708PB Wageningen, The Netherlands. E-mail: jan.kammenga@wur.nl; and l.b.snoek@uu.nl

Here we go beyond mutant screens of *let-60(gf)* in a single genetic background in *C. elegans* by incorporating the effects of multiple genetic backgrounds. This provides the opportunity to explore the genetic variation for identifying novel modifiers of the Ras/MAPK pathway. We recently mapped modifiers affecting Ras/MAPK signaling associated with vulval development in a population of recombinant inbred lines derived from a cross between wild-type Hawaiian CB4856 and Bristol N2 (Schmid *et al.* 2015). The lines were sensitized by introgression of the G13E gain-of-function mutation (*n1046*) in the Ras gene *let-60* [mutation introgression recombinant inbred lines (miRILs)]. This mutation is analogous to mutations causing excess cell division in human tumors (Kyriakakis *et al.* 2015). Hawaiian CB4856 males were crossed with Bristol N2 *let-60* mutants. Random segregation of the two parental genomes was allowed, except for the *let-60* mutation which was kept homozygous from the F2 generation onwards. After 10 generations of self-fertilization, to drive all regions to homozygosity, independent miRILs were successfully obtained, each carrying the mutation. Quantitative trait loci (QTL) analysis on the vulval index (VI) of these miRILs in combination with allele-swapping experiments revealed the polymorphic monoamine oxidase A (MAOA) gene *amx-2* as a negative regulator of Ras/MAPK signaling (Schmid *et al.* 2015).

Here, we extended the study by Schmid *et al.* (2015) by studying the transcriptional architecture of the same *let-60(gf)*-sensitized miRILs. First, we measured the transcriptome of 33 miRILs using microarrays. Second, to gain further insight into the underlying molecular mechanisms, pathways, and new modifiers, we mapped gene expression QTL (eQTL). eQTL are polymorphic loci underlying variation in gene transcript abundances and can be used to detect loci which affect many transcript levels and transcriptional pathways (Jansen and Nap 2001). We found that the *let-60(gf)* mutation mainly reveals novel *trans*-eQTL, which are eQTL distant from the regulated gene. In contrast, *cis*-eQTL, genes that colocalize with the eQTL, were mostly independent of the *let-60(gf)* mutation. Of the *trans*-eQTL, 77 genes have an eQTL in a *trans*-band (eQTL hotspot) colocalizing with *amx-2*. Comparing the transcriptional profiles of transgenic lines with the N2 *amx-2* allele with the CB4856 *amx-2* allele showed the involvement of *amx-2* in 79% (61/77) of the genes mapping to this locus. Through network-assisted gene expression analysis, we found evidence that *amx-2* indirectly affects gene expression mapping to this *trans*-band.

MATERIALS AND METHODS

General methods and strains used

The strains MT2124 [N2 background with the *let60(n1046)* gain-of-function mutation] and CB4856 were used, as were 33 miRILs described previously (Schmid *et al.* 2015). A file with the strains and the genetic map has been included (Supplemental Material, Table S1). Furthermore, transgenic lines *amx-2(lf);Si[amx-2(Bristol)];let-60(gf)* and *amx-2(lf);Si[amx-2(Hawaii)];let-60(gf)* containing the N2 or CB4856 allele of *amx-2* in a *amx-2*(lf);*let-60*(gf) background were used in a confirmation experiment. For details regarding the construction of these lines, see Schmid *et al.* (2015).

Strains were maintained on NGM agar seeded with OP50 bacteria at 20°, strains were age synchronized by bleaching and were harvested 72 hr postsynchronization. One sample consisted of multiple pooled, nonstarved populations from approximately four separate 9-cm NGM plates.

RNA isolation, cDNA synthesis, and cRNA synthesis

The RNA of the samples was isolated using the RNEasy Micro Kit from Qiagen (Hilden, Germany), following the "Purification of Total RNA from Animal and Human Tissues" protocol with a modified lysing procedure. As prescribed, 150 μl RLT buffer and 295 μl RNAse-free water were used to lyse the samples, but with an addition of 800 μg/ml proteinase K and 1% β-mercaptoethanol. This suspension was incubated for 30 min at 55° and 1000 rpm in a Thermomixer (Eppendorf, Hamburg, Germany). Thereafter the protocol as supplied by the manufacturer was followed.

For gene expression analysis, 200 ng of RNA (as quantified by NanoDrop) was used in the "Two-Color Microarray-Based Gene Expression Analysis; Low Input Quick Amp Labeling" protocol, version 6.0, from Agilent (Agilent Technologies, Santa Clara, CA).

Microarray hybridization and scanning

The Agilent *C. elegans* (V2) Gene Expression Microarray 4X44K slides were used to measure gene expression. As recommended by the manufacturer, the samples were hybridized for 17 hr and scanned by an Agilent High Resolution C Scanner. The intensities were extracted using Agilent Feature Extraction Software (version 10.7.1.1). The data were normalized using the Limma package in "R" (version 3.3.0 x64). For within-array normalization, the "Loess" method was used and the "Quantile" method for between-array normalization (Zahurak *et al.* 2007; Smyth and Speed 2003). Unless mentioned otherwise, the $\log_2$ transformed intensities were used in subsequent analysis.

Expanding the genetic map

Previously, the strains were genotyped with 73 fragment length polymorphism (FLP) markers (as described in Schmid *et al.* 2015 and Zipperlen *et al.* 2005) (Table S2).

To increase the resolution of the genetic map, *cis*-eQTL of a large *C. elegans* eQTL experiment were used to further pinpoint the crossovers (Rockman *et al.* 2010). The gene expression of the miRILs was transformed to the mean of the two parental lines (R) by

$$R_{x,i} = \frac{Y_{x,i}}{0.5 \times \left(Y_{MT2124,i} + Y_{CB4856,i}\right)},$$

where Y stands for the untransformed intensities of strain x and spot i (1, 2, 3, ..., 45220). The obtained values were correlated to the *cis*-eQTL effects from Rockman *et al.* (2010). Since the current study uses a newer version of the *C. elegans* microarray, only the spots that occurred in both designs were compared. The expression markers were generated following a procedure that is a variation of the method described in West *et al.* (2006). Per 20 consecutive *cis*-eQTL, the correlation between the N2-eQTL effect and the transformed intensities (R) were calculated. In this way, the correlation would be negative if the genotype stemmed from CB4856, and positive if the genotype stemmed from N2.

In this way, 424 gene expression markers were generated per strain. To control for quality, the markers were filtered for calling the correct genotype in the four MT2124 replicas, the four CB4856 replicas, and in >50% of the samples an absolute correlation >0.5 was required. This pruning resulted in 204 reliable gene expression markers. The quality of these markers was controlled by predicting the genotype by expression in RIL AH2244, in which the gene expression was measured twice. There, we found that 10/204 selected gene expression markers were in disagreement with the genotype. This could be reduced to 0 by comparing only markers with an absolute correlation >0.6. Therefore, all the correlations with an absolute value >0.6 were assigned the predicted marker, which corresponds to an error rate of <0.01 per strain. The genotypes of the remaining markers were manually inferred from the surrounding markers. Furthermore, the genotypes at the ends of the chromosomes were inferred from the distal

most-assigned marker. This brings the size of the resulting map to 289 markers. The correlations and assigned genotypes can be found in Table S3.

Evaluating the genetic map

The 289 marker set was analyzed by correlation analysis for markers describing unique crossover events and to see if there are any strong linkages between chromosomes (Figure S1). This led to the selection of 247 markers indicating the border of a crossover event. To reduce the chances of false positives, we only used markers where the frequency of the least-occurring genotype in the population was >15%. It has to be noted that this excluded most of chromosome IV [as the genotype was predominantly N2 due to selection for strains including the *let-60(gf)* mutation (Schmid *et al.* 2015)]. Furthermore, also the *peel-1/zeel-1* region on chromosome I was excluded for the same reason (Seidel *et al.* 2008).

eQTL mapping and threshold determination

Mapping of eQTL mapping was done in "R" (version 3.3.0 x64) and the gene expression data were fitted to the linear model

$$y_{i,j} \sim x_j + e_j,$$

where y is the $\log_2$-normalized intensity as measured by microarray of spot i ($i = 1, 2, ..., 45220$) of miRIL j. This is explained by the genotype (either CB4856 or N2) on marker location x ($x = 1, 2, ..., 247$) of miRIL j.

A permutation approach was used to determine an empirical false discovery rate (Snoek *et al.* 2017; Vinuela *et al.* 2010). First, the $\log_2$-normalized intensities were randomly distributed per gene over the genotypes. This randomized data set was tested using the eQTL mapping model. This procedure was repeated 10 times. The threshold was determined using

$$\frac{\text{FDS}}{\text{RDS}} \leq \frac{m_0}{m} q \cdot \log(m),$$

where, at a specific significance level, the false discoveries (FDS) were the averaged outcome of the permutations and read discoveries (RDS) were the outcome of the eQTL mapping. The value of m_0, the number of true null hypotheses tested, was 45220 RDS; and for the value of m, the number of hypotheses tested, the number of spots (45220) was taken. Because this study only used a limited set of strains, a more lenient threshold of 0.1 was taken as the q-value (Benjamini and Yekutieli 2001), which resulted in a threshold of $-\log_{10}(p) > 3.2$.

Statistical power calculations

The statistical power of the mapping was determined at the significance threshold of $-\log_{10}(p) > 3.2$. Using the genetic map (33 strains with 247 markers), 10 QTL were simulated per marker location, explaining 20–80% of the variation (in increments of 5%). Next to a peak, random variation was also introduced, based on a standard normal distribution ($\mu = 0$ and $\sigma = 1$). Peaks with corresponding explanatory power were simulated in this random variation (*e.g.*, a peak size of 1 corresponds to 20% explained variation). Furthermore, random data without peaks was also generated. These simulated data were mapped as described above and for each simulated peak it was determined: (i) if it was detected correctly, (ii) how precise the effect size estimation was, and (iii) how precise the location determined was. An overview of the results can be found in Table S4.

eQTL analysis

The distinction between *cis*- and *trans*-eQTL was made on the distance between the gene and the eQTL peak. Given the relatively low number of unique recombinations (due to the limited set of strains), the *cis*-eQTL window was set at 2 Mb. This means that if a gene lies within 2 Mb of the QTL peak or the confidence interval, it is called a *cis*-eQTL. The confidence interval was based on a $-\log_{10}(p)$ drop of 1.5 compared to the peak.

Trans-bands were identified based on a Poisson distribution of the mapped *trans*-eQTL (as in Rockman *et al.* 2010). The number of *trans*-eQTL was counted per 1-Mb bin, leading to the identification of 52 bins with *trans*-eQTL. Since we mapped 1149 *trans*-eQTL peaks (spots) to 52 bins, we expected 22.10 *trans*-eQTL per bin with *trans*-eQTL assigned to it. Based on a Poisson distribution, any bin linking >30 spots with a *trans*-eQTL would have a significance of $P < 0.05$, and >38 *trans*-eQTL would yield a significance of $P < 0.001$. In this way, six *trans*-band loci were identified.

Comparative analysis against previous eQTL experiments was done on remapped experiments downloaded from WormQTL (Snoek *et al.* 2013; van der Velde *et al.* 2014) and EleQTL (http://www.bioinformatics.nl/EleQTL). This data set consists of four different experiments representing nine different conditions. The first set contains eQTL in two temperature conditions, 16° and 24°, measured in the L3 stage (Li *et al.* 2006). The second set contains eQTL over three life stages: L4 juvenile animals grown at 24°, reproducing adult animals (96 hr) grown at 24°, and aging animals (214 hr) grown at 24° (Vinuela *et al.* 2010). The third set contains eQTL from a single experimental condition (young adults grown at 20°) measured on a large RIL panel (Rockman *et al.* 2010). The fourth set contains eQTL from three experimental conditions over the course of a heat-shock treatment: a control condition (L4 animals grown for 48 hr at 20°), a heat-shock condition (L4 animals grown for 46 hr at 20° and exposed to 2 hr of 35°), and a recovery condition (similar to heat shock, only followed by 2 hr at 20°) (Snoek *et al.* 2017). Each of these experiments was compared at FDR = 0.05 to the eQTL mapped at FDR = 0.10 in the *let-60(gf)*-sensitized miRILs.

Since the data set of Rockman *et al.* (2010) was used for expanding the genetic map, analysis was also conducted excluding this study. The reason for excluding this set from analysis was that a bias could be introduced in overlap with the *cis*-eQTL. The main conclusion that *cis*-eQTL are less unique than *trans*-eQTL also stands with this analysis. Excluding the Rockman *et al.* data, resulted in detection of 999/1516 (65.9%) *cis*-eQTL and 171/898 (19.0%) *trans*-eQTL present in previous experiments.

Enrichment analysis

Gene group enrichment analysis was done using a hypergeometric test on the unique genes (not on the spots) with the following criteria: Bonferroni-corrected $P < 0.05$; size of the category, $n > 3$; and size of the overlap, $n > 2$.

The following databases were used: the WormBase (www.wormbase.org) WS220 gene class annotations, WS256 GO-annotation, anatomy terms, phenotypes, RNAi phenotypes, developmental stage expression, and disease-related genes (Harris *et al.* 2014); the MODENCODE release 32 transcription-factor binding sites (www.modencode.org; Gerstein *et al.* 2010; Niu *et al.* 2011), which were mapped to transcription start sites (according to Tepper *et al.* 2013); and the KEGG (Kyoto Encyclopedia of Genes and Genomes) pathway release 65.0 (www.genome.jp/kegg/) (Ogata *et al.* 1999).

amx-2 allelic comparison

Four independent transgenic lines, two of *amx-2(lf);Si[amx-2(Bristol)];let-60(gf)* and two of *amx-2(lf);Si[amx-2(Hawaii)];let-60(gf)*, were used to investigate the effect of the *amx-2* CB4856 and N2 allele on gene expression. These lines contain single-copy insertions on LGII of the N2 or

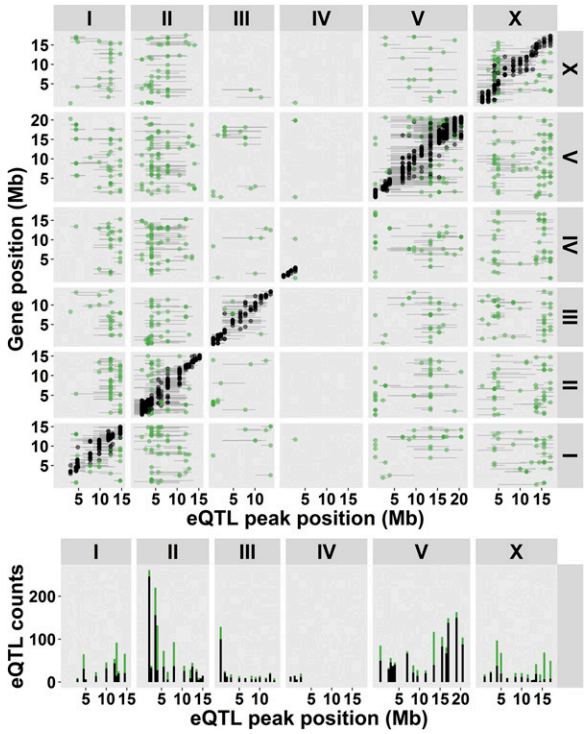

Figure 1 eQTL mapping in the *let-60(gf)* miRIL population. On top, the *cis-trans* plot is shown. On the horizontal axes, the positions of the eQTL are plotted along the six chromosomes. The location of the genes with an eQTL is plotted on the vertical axis. The black ●'s represent *cis*-eQTL (lying within 2 Mb of the regulated gene), the green ●'s represent *trans*-eQTL (eQTL lying elsewhere). The gray horizontal lines indicate the confidence interval of the QTL location [based on a 1.5 drop in $-\log_{10}$ (p)]. The bottom histogram shows the number of eQTL per genomic location. Note that on chromosome IV, hardly any eQTL are mapped, this is because of linkage of the *let-60(gf)* mutation (which is located at IV: 11.7 Mb).

CB4856 alleles of *amx-2* in an N2 *amx-2*(lf); *let-60*(gf) background. The effect of different alleles on gene expression was measured by microarray for each independent transgenic line and compared to the effects of the eQTL mapping to the *trans*-band closest to the position of *amx-2*.

Connectivity network analysis

To investigate the connectivity and function of the affected genes we used WormNet (version 3) (Cho *et al.* 2014) and GeneMANIA plug-in for Cytoscape (version 3.4.0) (Montojo *et al.* 2010; Shannon *et al.* 2003). WormNet was used to investigate enrichment in connectivity within groups of genes. For example, groups of coexpressed genes mapping to the same *trans*-band were assumed to share the same regulator. Further evidence for this coexpression and regulation can be found in WormNet if these genes are significantly more connected than by chance. GeneMANIA was used to find the closest neighbors, those genes with the most connections, of *amx-2* and *let-60* to locate the genes by which *amx-2* modifies RAS signaling.

Data availability

All strains used can be requested from the authors. The transcriptome data sets generated and the mapped eQTL profiles can be interactively accessed via http://www.bioinformatics.nl/EleQTL. Moreover, the raw transcriptomic data are also available at ArrayExpress (E-MTAB-5856).

Table 1 The number of genes with an eQTL

eQTL effect	*cis*-eQTL	*trans*-eQTL
N2 higher	1074 (1564)	448 (582)
CB4856 higher	456 (632)	464 (576)
Total[a]	1516 (2196)	898 (1149)

The numbers in brackets indicate the number of spots.
[a]The discrepancy between the sum of N2 higher, CB4856 higher, and the total is due to genes being represented by multiple spots, which often represent different splice variants.

RESULTS

eQTL mapping in miRIL population

Using microarrays, we measured gene expression levels in 33 miRILs sensitized for RAS/MAPK signaling by introgression of a *let-60* (gf) mutation in a segregated N2/CB4856 genetic background (Figure S2) (Schmid *et al.* 2015). Analysis of the statistical power of this population with a genetic map of 247 informative markers showed that we can detect 77% of the QTL explaining 40% of the variation (Table S4). We detected 2303 genes (represented by 3226 array spots) with at least one eQTL (FDR = 0.1, $-\log_{10}(p) > 3.2$; Figure 1, Table 1, and Table S5). For 1516 of these genes, a *cis*-eQTL was found, indicating regulation from within a window of 2 Mb around the affected gene. For 898 genes a *trans*-eQTL was found, showing regulation more distal from the affected transcript. Most *cis*-eQTL (1074 out of 1516; ~71%) show a positive effect for the N2 allele; whereas for the *trans*-eQTL, the positive and negative effects were equally distributed over the N2 and CB4856 allele (Table 1).

The eQTL were not equally distributed across the genome. We detected different clustered *trans*-eQTL as "hotspots" or *trans*-bands. *Trans*-bands are frequently found in eQTL experiments and indicate a locus with one or multiple alleles affecting the expression of many distant genes. To identify the *trans*-bands in our experiment, we calculated the chance of overrepresentation of *trans*-eQTL per marker, using a Poisson distribution (as in Rockman *et al.* 2010). This method was applied per 1-Mb window on the genome. The *trans*-bands that were identified in adjacent windows were merged. This way, six *trans*-bands were identified (Poisson distribution, $P < 0.001$; Table 2).

Specificity of let-60 eQTL

By comparative analysis of different environments and/or populations, it has been shown that eQTL *trans*-bands can be population, environment, or age specific (for example, see Li *et al.* 2006). To investigate if and which eQTL are specifically found in the sensitized miRILs, we compared the detected eQTL to the eQTL found in nonsensitized RILs (Li *et al.* 2006; Rockman *et al.* 2010; Vinuela *et al.* 2010; Snoek *et al.* 2017). These data sets contain eQTL mapped over nine different conditions (see *Materials and Methods*), which were compared at an FDR = 0.05 with the eQTL mapped in the sensitized miRILs. We found that ~73% (1112 out of 1516) of the genes with a *cis*-eQTL in the miRIL population were also found in one or more of the previous studies (Figure 2 and Figure S3B). When taking the allelic effects into account, of the 1074 genes with a *cis*-eQTL that gave a higher expression linked to the N2 allele, 816 (~76%) were found in other studies. For the 456 genes with a *cis*-eQTL that gave a higher expression linked to the CB4856 allele, 310 (~68%) were found in other studies. This shows that the majority of the *cis*-eQTL detected in the miRIL population can be also be detected in other experiments.

In contrast, for the *trans*-eQTL detected in our experiment, not taking location into account, we only found ~24% (214 out of 898) of the genes had a *trans*-eQTL in at least one of the previous experiments (Figure 2

Table 2 *Trans*-bands detected in the sensitized miRILs

Trans-band Position	Number of Genes with a *Trans*-eQTL (spots)	Detected in Previous Experiments[a]	Uniqueness[b]
I: 12.0–15.0 Mb	107 (127)	9/107 (8.4%)	$P = 1.6 \times 10^{-4}$
II: 3.0–6.0 Mb	166 (205)	6/166 (3.6%)	$P = 4.1 \times 10^{-11}$
II: 7.0–8.0 Mb	45 (56)	0/45 (0%)	$P = 6.7 \times 10^{-6}$
V: 13.0–14.0 Mb	70 (77)	0/70 (0%)	$P = 4.5 \times 10^{-8}$
X: 4.0–5.0 Mb	87 (107)	3/87 (3.4%)	$P = 1.7 \times 10^{-6}$
X: 15.0–17.0 Mb	85 (104)	1/85 (1.2%)	$P = 3.4 \times 10^{-8}$

[a] Based on Li *et al.* (2006), Vinuela *et al.* (2010), Rockman *et al.* (2010), and Snoek *et al.* (2017); if the same gene had an eQTL on the same chromosome.
[b] Based on a Poisson distribution, where it was expected that 23.8% of the *trans*-eQTL were replicated. *P*-value indicates the likeliness of an overrepresentation of *trans*-eQTL in the miRIL population.

and Figure S3C). To further compare the *trans*-eQTL overlap, it was investigated whether the *trans*-eQTL colocalized on the same chromosome. Using that criterion, ~9% (80 out of 898) of the genes with a *trans*-eQTL were found in a previous study. This showed that the majority of the genes with a *trans*-eQTL were specifically detected in the sensitized miRIL population. This observation also extended to the *trans*-bands. To test the specificity of the *trans*-bands, we counted the number of times a gene within the miRIL *trans*-bands had a colocating *trans*-eQTL in other studies. All *trans*-bands were found to be specific for the *let-60(gf)* miRILs (Poisson distribution, $P < 0.001$; Table 2). This provides additional evidence that these *trans*-bands are specific for interaction between the genetic background and the *let-60(gf)* mutation.

Altogether, we identified 404 genes with a novel *cis*-eQTL and 684 genes with a novel *trans*-eQTL (Figure 3A). As our method can be biased by the way the genetic map was constructed (using expression differences, see *Materials and Methods*), we conducted the same analyses using the original FLP map. Our conclusions on the detection of novel *cis*- and *trans*-eQTL were not affected by the different genetic map (for details, see File S1). This implies that a substantial majority of *trans*-eQTL showed a mutation-dependent induction. This is also illustrated by showing the eQTL that were consistently found (Figure 3B), which mainly shows the *cis*-diagonal- and a few *trans*-eQTL.

Functional allelic differences

Enrichment analysis on groups of genes with an eQTL mapping to the same *trans*-band can be used to uncover the functional consequences of the allelic variation at the selected locus. Enrichment analysis was done on GO-terms, KEGG, anatomy terms, disease phenotypes, development expression, phenotypes, transcription-factor binding sites, and RNAi phenotypes (Table S6).

The genes with *cis*-eQTL were enriched for genes in the gene classes *math*, *bath*, *btb*, and *fbx*. These classes contain many genes that function as intra- and extracellular sensors involved in gene–environment interactions, and were found highly polymorphic between N2 and CB4856, but also between other wild isolates (Thompson *et al.* 2015; Volkers *et al.* 2013). The genes with *trans*-eQTL with higher expression linked to CB4856 loci were enriched for genes related to development in general and gonad development specifically. These enrichments were likely to stem from the *trans*-bands on chromosome I: 12–15 Mb and II: 3–6 Mb specifically. These two *trans*-bands mainly consisted of genes with a higher expression linked to the CB4856 locus and were enriched for genes associated with reproduction and/or development.

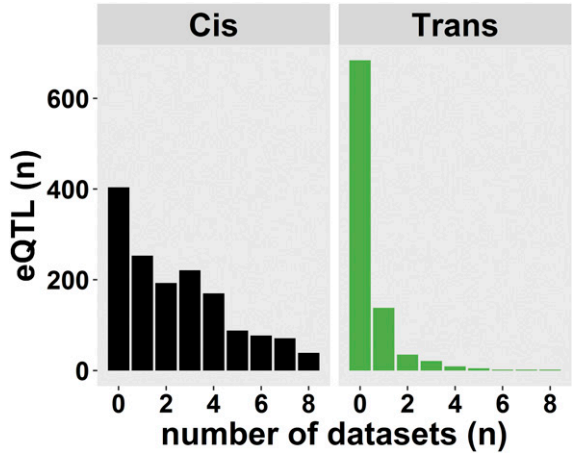

Figure 2 eQTL detected in previous experiments. The eQTL mapped in the *let-60(gf)* RIL population were compared to eQTL mapped in three published *C. elegans* eQTL studies, representing nine different conditions (Li *et al.* 2006; Rockman *et al.* 2010; Vinuela *et al.* 2010; Snoek *et al.* 2017). The histogram shows how many of the eQTL mapped in this study were found back in these independent conditions. Whereas the majority of *cis*-eQTL was mapped in previous studies, there was only a minority of *trans*-eQTL that had been mapped.

Allelic effect of amx-2 on gene expression

The *trans*-band on chromosome I: 12–15 Mb colocalizes with a previously identified QTL for vulval induction, for which *amx-2* was identified as polymorphic regulator (Schmid *et al.* 2015). To determine if the *trans*-eQTL mapping to the *amx-2* locus were affected by the allelic difference between N2 and CB4856, we measured gene expression in transgenic lines containing single-copy insertions of either allele of *amx-2* in a *amx-2(lf)*; *let-60(gf)* background. For each allele, two independent strains were created and the transcriptome was measured using microarrays (Schmid *et al.* 2015). From these measurements, the allelic effects of *amx*-2 on gene expression were determined and compared with the *trans*-eQTL effects measured in the miRIL population. These were found to correlate significantly (Figure S4; R^2 ~0.34; $P < 2 \times 10^{-8}$). Specifically, 61 of the 77 genes with an eQTL colocalizing with *amx-2* showed the same allelic effect in the transgenic strains carrying the two *amx-2* variants. Furthermore, analysis of the effect directions showed that the *trans*-band on chromosome I (Table 2) consists of two separate *trans*-bands (see Figure S4); the first colocalizing with *amx-2* and the second lying more distal on chromosome I.

To further investigate the mechanism by which *amx-2* modifies *let-60* Ras/MAPK signaling, we used the well-established *C. elegans* connectivity networks WormNet (Cho *et al.* 2014) and GeneMANIA (Montojo *et al.* 2010; Shannon *et al.* 2003). WormNet showed that the genes mapping to the *amx-2* locus were more connected than expected by chance ($P < 3 \times 10^{-13}$). Visualizing the connectivity of these genes together with *amx-2* and *let-60* using GeneMANIA identified one major gene cluster (Figure 4). As expected, genes affected by the *trans*-band were found to be highly connected and at the core of the cluster, indicating a shared biological function. In contrast, 25% of the genes with a *cis*-eQTL at the *trans*-band location were not connected, and those that were connected had only one to three connections. Interestingly, *let-60* was at the core of the cluster of genes with a *trans*-eQTL, whereas *amx-2* was at the periphery. We found six genes, *lin-40* (also called *egr-1*), *egl-27*, *trr-1*, *pbrm-1*, *ceh-26* (also called *pros-1*), and *emb-5*, that were previously found to have a genetic interactions

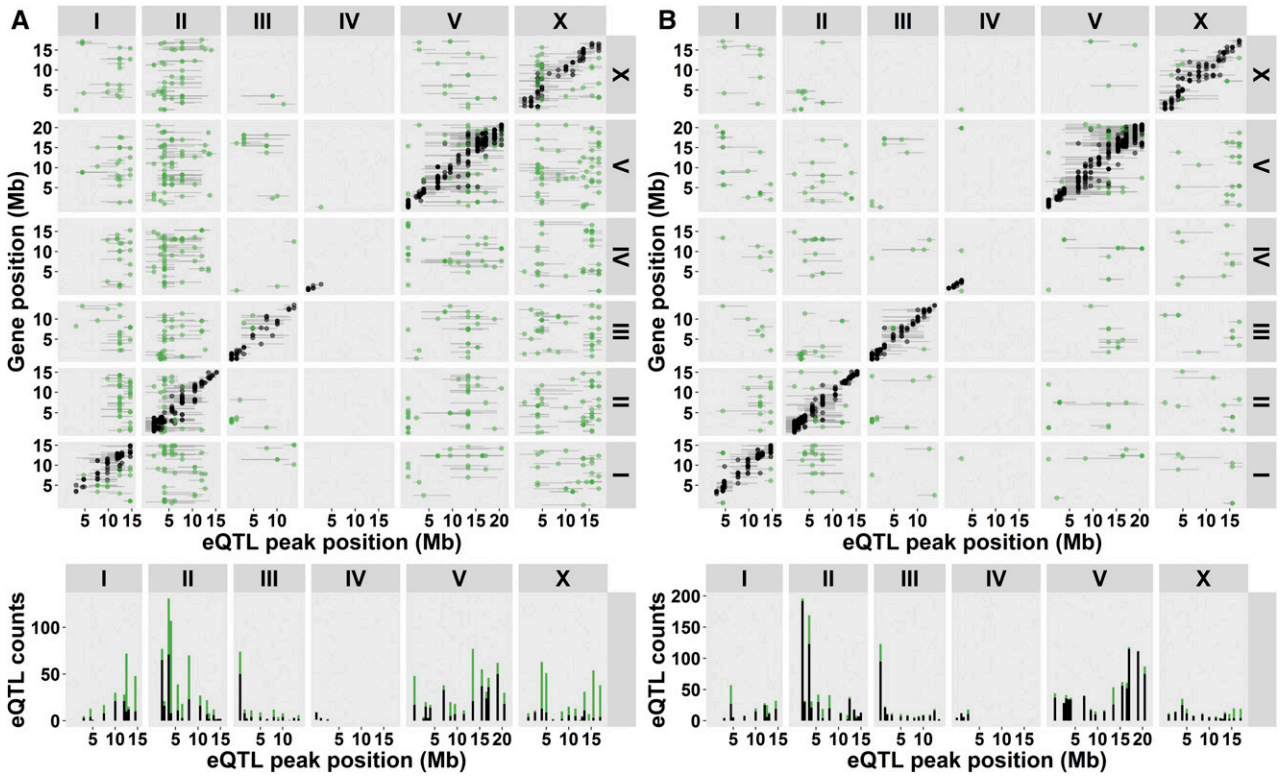

Figure 3 eQTL mapped in the *let-60(gf)* miRIL population compared to other studies (Li *et al.* 2006; Rockman *et al.* 2010; Vinuela *et al.* 2010; Snoek *et al.* 2017). As in Figure 2, the *cis*- and *trans*-eQTL are plotted. (A) eQTL only found in the miRIL population. (B) eQTL found over multiple studies.

with *let-60* (Lee *et al.* 2010; Lehner *et al.* 2006; Byrne *et al.* 2007). These could be the genes through which *amx-2* affects RAS/MAPK signaling.

DISCUSSION

Ras/MAPK signaling is strongly affected by gain-of-function mutations in *let-60*, as shown by the strong effect on vulva development in *C. elegans* (Beitel *et al.* 1990). The allele *let-60(n1046)* hyper-activates Ras/MAPK signaling, leading to a multivulva phenotype and the differentiation of more than three vulval precursor cells. In the miRIL population, which carries a *let-60(n1046)* mutation in a segregating N2/CB4856 background, a wide range of VI was found. While in the full N2 background, VI of the *let-60(gf)* mutation was 3.7 induced vulval cells on average, the VI in the miRIL population varied from 3.0 to 5.7 induced vulval cells, illustrating the strong modulatory effect of the genetic background on the mutant phenotype (Schmid *et al.* 2015). By measuring gene expression across the different miRILs, we gained insight into the genetic background effects on the transcriptional architecture of *let-60(gf)*-sensitized miRILs.

The let-60(gf) mutation affects gene expression in trans

To our knowledge, this is the first study where a mutation, introgressed into a panel of RILs, is used to investigate the genetic architecture of transcript variation by eQTL analysis. Unfortunately, the direct effect of the *let-60(gf)* allele on the genetic background is impossible to determine in this population, since there is no population with the same genetic background lacking the *let-60(gf)* mutation. Therefore, we used previously published eQTL studies in *C. elegans* as an estimation for the miRIL-specific eQTL. We found that introgression of *let-60(gf)* leads to an overrepresentation of specific *trans*-eQTL, while the *cis*-eQTL showed a high overlap with eQTL observed in the absence of *let-60(gf)* allele. Although our study is based on a relatively small number of strains, the verification of identified eQTL against other eQTL studies in *C. elegans* shows that at least 73% of the identified *cis*-eQTL were previously discovered. This supports our power analysis, showing that our study has enough statistical power to detect eQTL with larger effects.

Given that *cis*-eQTL are most likely genes with polymorphisms in or near the gene itself, it is expected that most have been previously discovered. In support of this, most of the *cis*-eQTL genes show higher expression in N2, making it likely that a relatively large proportion of these *cis*-eQTL indeed stem from polymorphisms causing mishybridization on the microarrays instead of true expression differences (Rockman *et al.* 2010; Alberts *et al.* 2007). Therefore, most of the *cis*-eQTL will not represent gene expression changes that can be linked to the *let-60(gf)* mutation in the miRIL population. That is also exactly what we found when constructing the regulatory network by connecting *cis*- and *trans*-eQTL to *let-60*; *cis*-eQTL are only loosely, or not at all, connected to the network.

Compared to *cis*-eQTL, the *trans*-eQTL identified in the miRIL population were hardly found in previous eQTL studies in *C. elegans* (only 24% were previously detected). However, it should be noted that *trans*-eQTL are themselves are also environment and age dependent (Vinuela *et al.* 2010; Francesconi and Lehner 2014; Li *et al.* 2006; Snoek *et al.* 2017), therefore it is possible that not all the *trans*-eQTL are indeed *let-60* induced. For example, they might be age related (Vinuela *et al.* 2010). Another aspect that influences detection of *trans*-eQTL is the power of the study, as *trans*-eQTL explain less of the variation than *cis*-eQTL. However, by being stringent in the overlap (requiring only one match over nine different environments), it is likely that most of these eQTL would be detected. This makes it likely that many of the identified *trans*-eQTL are specifically linked to an effect of the *let-60(gf)* mutation in the genetic background. This extends the idea that environmental

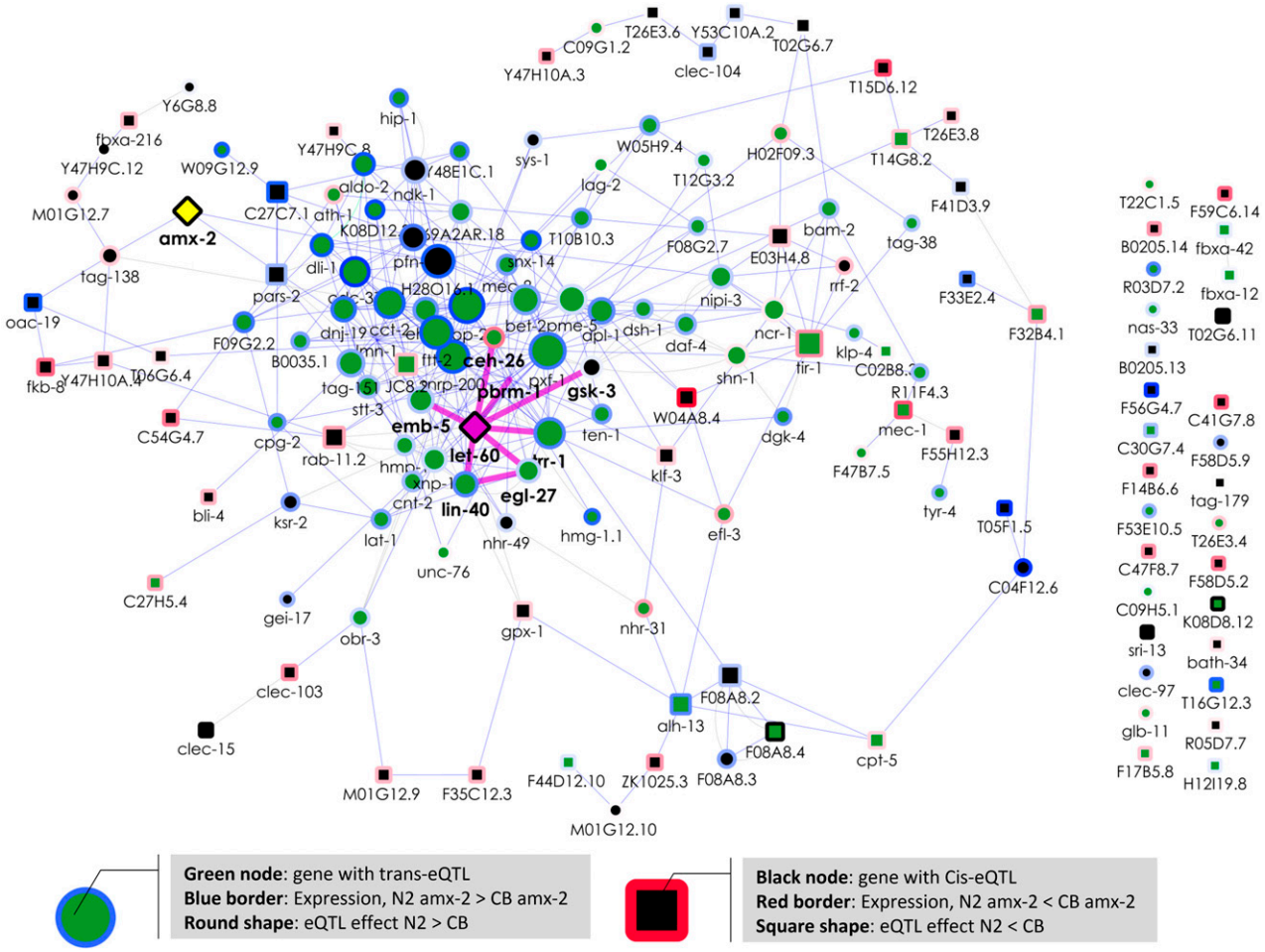

Figure 4 Interaction network of genes colocalizing with *amx-2*. Genes with an eQTL colocalizing with *amx-2* were selected together with *amx-2* (yellow) and *let-60* (pink). Interactions were obtained from GeneMANIA (Montojo *et al.* 2010; Shannon *et al.* 2003). Node color indicates *cis* in black and *trans* in green. Node shape indicates eQTL effect, N2 > CB4856 as a ○ and CB4856 > N2 as a □. Node border color gradient indicates expression in *amx-2* transgenic lines (blue N2-*amx-2*-allele > CB4856-*amx-2* allele, red CB4856-*amx-2* allele > N2 *amx-2* allele). Node size indicates number of edges connected. Edges in blue show coexpression links and edges in pink show genetic interactions as found by Lee *et al.* (2010), Lehner *et al.* (2006), and Byrne *et al.* (2007). Genes connected by genetic interactions have boldface gene names (as well as *amx-2*).

perturbations can reveal additional genetic variation (Li *et al.* 2008) by perturbing the genetic environment (Kammenga *et al.* 2008; Duveau and Felix 2012; Schmid *et al.* 2015). The advantage of mutational perturbation and perturbation via induced responses in eQTL studies (for example, see Snoek *et al.* 2012 and Snoek *et al.* 2017) is that it contextualizes the transcriptional response. Yet, as the phenotypic influence of *let-60(gf)* in the miRIL population was investigated before, we know it results in a phenotype. In the study presented here, the context is the *let-60(gf)* mutation, which results in a phenotype where VI is affected. It is therefore interesting that the *trans*-bands colocalize with QTL mapped for VI in the same miRIL population: *trans*-band I: 12–15 Mb overlaps with QTL1b, *trans*-band II: 7–8 Mb with QTL2, and *trans*-band V: 13–14 Mb with QTL3 (Schmid *et al.* 2015). This colocalization adds to the plausibility that the novel *trans*-eQTL detected in the miRIL population are indeed due to the *let-60(gf)* mutation and its interaction with the genetic background.

A trans-band on chromosome I links to variation in the amx-2 gene

Using the same *let-60(gf)* miRIL population, we have previously identified the polymorphic MAOA *amx-2* as a background modifier that negatively regulates the Ras/MAPK pathway and the VI phenotype (Schmid *et al.* 2015). The *trans*-band on chromosome I colocalizes with the *amx-2* QTL for VI [QTL1b (Schmid *et al.* 2015)], it is therefore possible that the modifier *amx-2* also affects gene expression. More specifically, the *trans*-band on chromosome I originally identified in the miRILs consists of two separate regulatory loci. The N2 allelic effect at the *amx-2* locus is mostly negative; whereas for the more distal part of the original *trans*-band, the N2 allelic effect is mostly positive. Yet, it seems unlikely that *amx-2* is a direct gene expression effector. As *amx-2* is a mitochondrial MAOA, a catalyzer of neuropeptide oxidative deamination, it will probably not influence gene expression directly (Tipton *et al.* 2004). Placing the *trans*-eQTL of the *amx-2* *trans*-band in a gene interaction network supports this line of reasoning: although *let-60* is in the center of the *trans*-eQTL, *amx-2* is only peripheral.

By measuring gene expression in transgenic lines expressing the N2 or CB4856 allelic variants of *amx-2* in an *amx-2(lf);let-60(gf)* genetic background, we attempted to link the allelic effect of *amx-2* to the *trans*-eQTL mapping to the *amx-2* locus. As a significant correlation between the expression differences in the transgenic lines and the *trans*-eQTL effects mapping to the *amx-2* locus is found, these *trans*-eQTL can be confidently linked to allelic variation in *amx-2*. As discussed

before, it is unlikely that *amx-2* is the direct cause of the transcriptional variation, but rather it acts through an indirect mechanism. One route of effect might be through *amx-2*-mediated degradation of serotonin (5-HT) to 5-HIAA, which both affect VI (as discussed in Schmid *et al.* 2015). Subsequently, the affected VI might result in different gene expression levels. It is interesting to remark that the *amx-2* *trans*-band is characterized by downregulation of expression related to the N2 genotype as well as a decreased VI for that genotype.

As this places *amx-2* in the causal chain of events, we think it is most likely that *amx-2* does not affect gene expression directly but via another gene involved in Ras/MAPK signaling, possibly directly linked to *let-60*. Therefore, we hypothesize that *amx-2* affects Ras/MAPK signaling via one or more of the six previously found genes with a genetic interaction with *let-60*: *lin-40* (also called *egr-1*), *egl-27*, *trr-1*, *pbrm-1*, *ceh-26* (also called *pros-1*), and *emb-5*. For example, *egl-27* and *lin-40* both have a *trans*-eQTL mapping to the *amx-2* locus, and are the two MTA (metastasis-associated protein) homologs found in *C. elegans* (Ch'ng and Kenyon 1999; Herman *et al.* 1999; Solari *et al.* 1999). The proteins act in the NURD chromatin remodeling complex, which has previously been shown to antagonize Ras-induced vulval development (Solari and Ahringer 2000). Chromatin remodeling provides a more likely mechanism of action than the molecular role of *amx-2* itself.

Implications for understanding the Ras/MAPK pathway

How can our results help form a better understanding of the Ras/MAPK pathway? Our previous investigation on VI in the miRIL population resulted in the identification of three QTL harboring polymorphic Ras-signaling modifiers. Expanding our research to genetic variation affecting gene expression in a *let-60(gf)*-sensitized RIL population uncovered six *trans*-bands (or "eQTL hotspots"). As mentioned before, these *trans*-bands overlap with the QTL mapped for VI in Schmid *et al.* (2015). There are three more *trans*-bands that do not overlap with QTL for VI, but are also likely to represent modifier loci of the Ras/MAPK pathway, possibly underlying other Ras/MARK-associated phenotypic differences.

The main advantage of studying the genetic architecture of gene expression in the miRIL population is that it creates more insight in the genes and pathways affected by allelic variation acting on the Ras/MAPK pathway. It identifies hidden genetic variation; genetic variants that are unlocked under altered environmental conditions or when the genetic background is modified (for a review, see Paaby and Rockman 2014 and Kammenga 2017). Identification of background modifiers of disease pathways is important for gaining insight into individual-based differences of disease contraction. Mutant phenotypes can be strongly affected by the genetic background. For example, large variation in traits between different backgrounds in many different mutated genes has been observed in *C. elegans* (Paaby *et al.* 2015; Vu *et al.* 2015; Duveau and Felix 2012). A major discovery was that this variation in mutant phenotypes could be predicted from gene expression variation (Vu *et al.* 2015). These results are in line with the discovery of *trans*-bands at the location of each VI QTL. Furthermore, results presented here (and previously in Elvin *et al.* 2011) link variations in individual gene expression levels to enhancing or diminishing the severity of a Mendelian disorder caused by a so-called "major gene." More specifically, these differences seem to stem from a couple of modifier loci harboring polymorphic regulators.

So far, we only explored the *amx-2* *trans*-band, and it is likely that the other loci also contain polymorphic modifiers of the Ras/MAPK pathway. Genetic perturbation by *let-60(gf)* leads to a strong increase in specific *trans*-acting eQTL organized over six *trans*-bands, thus supporting the involvement of multiple genes as modifiers. Given the fact that we detected *amx-2* both via an indirect transcriptional response, but also mechanistically, we feel confident that the detected loci indeed harbor other modifiers. A single gene mutation apparently has the capacity to unlock a huge number of novel interactions controlled by many genes across different genetic backgrounds. Further studies should be conducted to identify and characterize these underlying polymorphic regulators.

Conclusion

Introgression of a mutation in a segregating genetic background allows for identification of polymorphic modifier loci. By introducing a *let-60(gf)* mutation in a N2/CB4856 genetic background, in the form of the miRIL population, and measuring the transcriptome, we identified six *trans*-bands specific for the *let-60(gf)* miRIL population. The majority of *trans*-eQTL are specific for the miRIL population, showing that genetic variation in gene expression can be specifically modified by a background mutation. Therefore, genetic perturbation can be viewed as analogous to environmental perturbation, which also results in specific *trans*-eQTL. We demonstrated the involvement of *amx-2* and the allelic variation between N2 and CB4856 in gene expression variation originating from chromosome I. Yet, we think it is unlikely that *amx-2* directly affects gene expression variation. Instead, we prefer the hypothesis that allelic variation in *amx-2* indirectly affects gene expression, possibly through the NURD complex.

ACKNOWLEDGMENTS

The authors thank Harm Nijveen for making our data available in EleQTL. M.R., T.S., A.H., and J.E.K. were funded by the European Community's Health Seventh Framework Program (FP7/2007-2013) under grant 222936. B.L.S. was funded by ERASysbio-plus ZonMW project GRAPPLE: Iterative modeling of gene regulatory interactions underlying stress, disease and ageing in *C. elegans* (project 90201066); and The Netherlands Organization for Scientific Research (project no. 823.01.001).

Author contributions: A.H., J.E.K., and B.L.S. conceived and designed the experiments. J.A.G.R., M.R., and T.S. conducted the experiments. M.G.S., L.v.B.v.d.P., and B.L.S. conducted transcriptome and main analyses. M.G.S., A.H., J.E.K., and B.L.S. wrote the manuscript.

LITERATURE CITED

Alberts, R., P. Terpstra, Y. Li, R. Breitling, J. P. Nap *et al.*, 2007 Sequence polymorphisms cause many false cis eQTLs. PLoS One 2: e622.

Beitel, G. J., S. G. Clark, and H. R. Horvitz, 1990 Caenorhabditis elegans ras gene let-60 acts as a switch in the pathway of vulval induction. Nature 348: 503–509.

Benjamini, Y., and D. Yekutieli, 2001 The control of the false discovery rate in multiple testing under dependency. Ann. Stat. 29: 1165–1188.

Byrne, A. B., M. T. Weirauch, V. Wong, M. Koeva, S. J. Dixon *et al.*, 2007 A global analysis of genetic interactions in Caenorhabditis elegans. J. Biol. 6: 8.

Chandler, C. H., S. Chari, D. Tack, and I. Dworkin, 2014 Causes and consequences of genetic background effects illuminated by integrative genomic analysis. Genetics 196: 1321–1336.

Ch'ng, Q., and C. Kenyon, 1999 egl-27 generates anteroposterior patterns of cell fusion in C-elegans by regulating Hox gene expression and Hox protein function. Development 126: 3303–3312.

Cho, A., J. Shin, S. Hwang, C. Kim, H. Shim *et al.*, 2014 WormNet v3: a network-assisted hypothesis-generating server for Caenorhabditis elegans. Nucleic Acids Res. 42: W76–W82.

Cowley, S., H. Paterson, P. Kemp, and C. J. Marshall, 1994 Activation of map kinase kinase is necessary and sufficient for Pc12 differentiation and for transformation of Nih 3t3 cells. Cell 77: 841–852.

Duveau, F., and M. A. Felix, 2012 Role of pleiotropy in the evolution of a cryptic developmental variation in Caenorhabditis elegans. PLoS Biol. 10: e1001230.
Elvin, M., L. B. Snoek, M. Frejno, U. Klemstein, J. E. Kammenga *et al.*, 2011 A fitness assay for comparing RNAi effects across multiple C. elegans genotypes. BMC Genomics 12: 510.
Francesconi, M., and B. Lehner, 2014 The effects of genetic variation on gene expression dynamics during development. Nature 505: 208–211.
Gerstein, M. B., Z. J. Lu, E. L. Van Nostrand, C. Cheng, B. I. Arshinoff *et al.*, 2010 Integrative analysis of the Caenorhabditis elegans genome by the modENCODE project. Science 330: 1775–1787.
Gokhale, R. H., and A. W. Shingleton, 2015 Size control: the developmental physiology of body and organ size regulation. Wiley Interdiscip. Rev. Dev. Biol. 4: 335–356.
Han, M., and P. W. Sternberg, 1990 let-60, a gene that specifies cell fates during C. elegans vulval induction, encodes a ras protein. Cell 63: 921–931.
Harris, T. W., J. Baran, T. Bieri, A. Cabunoc, J. Chan *et al.*, 2014 WormBase 2014: new views of curated biology. Nucleic Acids Res. 42: D789–D793.
Herman, M. A., Q. Ch'ng, S. M. Hettenbach, T. M. Ratliff, C. Kenyon *et al.*, 1999 EGL-27 is similar to a metastasis-associated factor and controls cell polarity and cell migration in C-elegans. Development 126: 1055–1064.
Jansen, R. C., and J. P. Nap, 2001 Genetical genomics: the added value from segregation. Trends Genet. 17: 388–391.
Jiang, H. S., and Y. C. Wu, 2014 LIN-3/EGF promotes the programmed cell death of specific cells in Caenorhabditis elegans by transcriptional activation of the pro-apoptotic gene egl-1. PLoS Genet. 10: e1004513.
Kammenga, J. E., 2017 The background puzzle: how identical mutations in the same gene lead to different disease symptoms. FEBS J. DOI:10.1111/febs.14080.
Kammenga, J. E., P. C. Phillips, M. De Bono, and A. Doroszuk, 2008 Beyond induced mutants: using worms to study natural variation in genetic pathways. Trends Genet. 24: 178–185.
Kyriakakis, E., M. Markaki, and N. Tavernarakis, 2015 Caenorhabditis elegans as a model for cancer research. Mol. Cell. Oncol. 2: e975027.
Lee, I., B. Lehner, T. Vavouri, J. Shin, A. G. Fraser *et al.*, 2010 Predicting genetic modifier loci using functional gene networks. Genome Res. 20: 1143–1153.
Lehner, B., C. Crombie, J. Tischler, A. Fortunato, and A. G. Fraser, 2006 Systematic mapping of genetic interactions in Caenorhabditis elegans identifies common modifiers of diverse signaling pathways. Nat. Genet. 38: 896–903.
Li, Y., O. A. Alvarez, E. W. Gutteling, M. Tijsterman, J. Fu *et al.*, 2006 Mapping determinants of gene expression plasticity by genetical genomics in C. elegans. PLoS Genet. 2: e222.
Li, Y., R. Breitling, and R. C. Jansen, 2008 Generalizing genetical genomics: getting added value from environmental perturbation. Trends Genet. 24: 518–524.
Mansour, S. J., W. T. Matten, A. S. Hermann, J. M. Candia, S. Rong *et al.*, 1994 Transformation of mammalian cells by constitutively active MAP kinase kinase. Science 265: 966–970.
Montojo, J., K. Zuberi, H. Rodriguez, F. Kazi, G. Wright *et al.*, 2010 GeneMANIA Cytoscape plugin: fast gene function predictions on the desktop. Bioinformatics 26: 2927–2928.
Niu, W., Z. J. Lu, M. Zhong, M. Sarov, J. I. Murray *et al.*, 2011 Diverse transcription factor binding features revealed by genome-wide ChIP-seq in C. elegans. Genome Res. 21: 245–254.
Ogata, H., S. Goto, K. Sato, W. Fujibuchi, H. Bono *et al.*, 1999 KEGG: kyoto encyclopedia of genes and genomes. Nucleic Acids Res. 27: 29–34.
Paaby, A. B., and M. V. Rockman, 2014 Cryptic genetic variation: evolution's hidden substrate. Nat. Rev. Genet. 15: 247–258.
Paaby, A. B., A. G. White, D. D. Riccardi, K. C. Gunsalus, F. Piano *et al.*, 2015 Wild worm embryogenesis harbors ubiquitous polygenic modifier variation. eLife 4: e09178.
Prior, I. A., and J. F. Hancock, 2012 Ras trafficking, localization and compartmentalized signalling. Semin. Cell Dev. Biol. 23: 145–153.
Rockman, M. V., S. S. Skrovanek, and L. Kruglyak, 2010 Selection at linked sites shapes heritable phenotypic variation in C. elegans. Science 330: 372–376.
Schmid, T., L. B. Snoek, E. Frohli, M. L. van der Bent, J. Kammenga *et al.*, 2015 Systemic regulation of RAS/MAPK signaling by the serotonin metabolite 5-HIAA. PLoS Genet. 11: e1005236.
Seidel, H. S., M. V. Rockman, and L. Kruglyak, 2008 Widespread genetic incompatibility in C. elegans maintained by balancing selection. Science 319: 589–594.
Shannon, P., A. Markiel, O. Ozier, N. S. Baliga, J. T. Wang *et al.*, 2003 Cytoscape: a software environment for integrated models of biomolecular interaction networks. Genome Res. 13: 2498–2504.
Smyth, G. K., and T. Speed, 2003 Normalization of cDNA microarray data. Methods 31: 265–273.
Snoek, B., M. Sterken, R. Bevers, R. Volkers, A. van't Hof *et al.*, 2017 Contribution of trans regulatory eQTL to cryptic genetic variation in C. elegans. BMC Genomics 18: 500.
Snoek, L. B., I. R. Terpstra, R. Dekter, G. Van den Ackerveken, and A. J. Peeters, 2012 Genetical genomics reveals large scale genotype-by-environment interactions in Arabidopsis thaliana. Front. Genet. 3: 317.
Snoek, L. B., K. J. Van der Velde, D. Arends, Y. Li, A. Beyer *et al.*, 2013 WormQTL–public archive and analysis web portal for natural variation data in Caenorhabditis spp. Nucleic Acids Res. 41: D738–D743.
Solari, F., and J. Ahringer, 2000 NURD-complex genes antagonise Ras-induced vulval development in Caenorhabditis elegans. Curr. Biol. 10: 223–226.
Solari, F., A. Bateman, and J. Ahringer, 1999 The Caenorhabditis elegans genes egl-27 and egr-1 are similar to MTA1, a member of a chromatin regulatory complex, and are redundantly required for embryonic patterning. Development 126: 2483–2494.
Tan, P. B., M. R. Lackner, and S. K. Kim, 1998 MAP kinase signaling specificity mediated by the LIN-1 Ets/LIN-31 WH transcription factor complex during C. elegans vulval induction. Cell 93: 569–580.
Tepper, R. G., J. Ashraf, R. Kaletsky, G. Kleemann, C. T. Murphy *et al.*, 2013 PQM-1 complements DAF-16 as a key transcriptional regulator of DAF-2-mediated development and longevity. Cell 154: 676–690.
Thompson, O. A., L. B. Snoek, H. Nijveen, M. G. Sterken, R. J. M. Volkers *et al.*, 2015 Remarkably divergent regions punctuate the genome assembly of the Caenorhabditis elegans Hawaiian strain CB4856. Genetics 200: 975.
Tipton, K. F., S. Boyce, J. O'Sullivan, G. P. Davey, and J. Healy, 2004 Monoamine oxidases: certainties and uncertainties. Curr. Med. Chem. 11: 1965–1982.
van der Velde, K. J., M. de Haan, K. Zych, D. Arends, L. B. Snoek *et al.*, 2014 WormQTLHD–a web database for linking human disease to natural variation data in C. elegans. Nucleic Acids Res. 42: D794–D801.
Vinuela, A., L. B. Snoek, J. A. Riksen, and J. E. Kammenga, 2010 Genome-wide gene expression regulation as a function of genotype and age in C. elegans. Genome Res. 20: 929–937.
Volkers, R. J., L. B. Snoek, C. J. Hubar, R. Coopman, W. Chen *et al.*, 2013 Gene-environment and protein-degradation signatures characterize genomic and phenotypic diversity in wild Caenorhabditis elegans populations. BMC Biol. 11: 93.
Vu, V., A. J. Verster, M. Schertzberg, T. Chuluunbaatar, M. Spensley *et al.*, 2015 Natural variation in gene expression modulates the severity of mutant phenotypes. Cell 162: 391–402.
West, M. A., H. van Leeuwen, A. Kozik, D. J. Kliebenstein, R. W. Doerge *et al.*, 2006 High-density haplotyping with microarray-based expression and single feature polymorphism markers in Arabidopsis. Genome Res. 16: 787–795.
Wu, Y., and M. Han, 1994 Suppression of activated Let-60 ras protein defines a role of Caenorhabditis elegans Sur-1 MAP kinase in vulval differentiation. Genes Dev. 8: 147–159.
Zahurak, M., G. Parmigiani, W. Yu, R. B. Scharpf, D. Berman *et al.*, 2007 Pre-processing Agilent microarray data. BMC Bioinformatics 8: 142.
Zipperlen, P., K. Nairz, I. Rimann, K. Basler, E. Hafen *et al.*, 2005 A universal method for automated gene mapping. Genome Biol. 6: R19.

Communicating editor: D-J. de Koning